Dry Metal Forming Open Access Journal

Fast Manuscript Track

Edited by Frank Vollertsen
Available online at elib.suub.uni-bremen.de

www.drymetalforming.de

Dry Met. Forming OAJ FMT 3 (2017) 030–040
Received 11 January 2017; published 1 February 2017

Analysis of tool-sided surface modifications for dry deep drawing of deep drawing steel and aluminum alloys in a model process

Jennifer Steiner[1*], Tom Häfner[2], Rong Zhao[3], Kolja Andreas[1], Michael Schmidt[2], Stephan Tremmel[3], Marion Merklein[1]

[1]Institute of Manufacturing Technology, Friedrich-Alexander-Universität Erlangen-Nürnberg, Egerlandstr. 13, 91058 Erlangen, Germany
[2]Institute of Photonic Technologies, Friedrich-Alexander-Universität Erlangen-Nürnberg, Konrad-Zuse-Str. 3/5, 91052 Erlangen, Germany
[3]Institute of Engineering Design, Friedrich-Alexander-Universität Erlangen-Nürnberg, Martensstr. 9, 91058 Erlangen, Germany

Abstract

The concept of sustainability motivates the development of energy-saving and low-polluting production processes. A sheet metal forming process without usage of lubricants is considered as one of these green production technologies. Forming processes without the need for traditional lubricants save process steps and additional costs to remove the remaining lubrication from the workpiece after forming. In order to realize such a dry forming process and to adjust the material flow effectively, tool surfaces were modified by amorphous carbon coatings and different surface finishing processes for roughness adjustment. To verify the general feasibility of the lubricant-free metal forming process, deep drawing of rectangular cups with and without lubrication with conventional forming tools was investigated. The dry deep drawing process was modelled numerically to analyze process parameters and identify critical contact conditions. By strip drawing tests, the tribological behavior of ta-C and a-C:H coated tools with different surface treatments was investigated. The deposition process and resulting properties of a-C:H coatings were further analyzed to improve their tribological performance. The effects of the process parameters – deposition temperature and bias voltage in the deposition chamber – were investigated using the one-factor-at-a-time method. The strip drawing tests revealed a high influence of the surface roughness of coated tools on the tribological behavior. Therefore, laser based smoothing was further investigated in this study. Laser radiation at 355 nm wavelength was applied as an effective and minimum heat-generating technique to remove the roughness asperities on ta-C coatings which are built during its growth. Finally, ta-C and a-C:H coatings were applied on tool surfaces and tested in a drawing process of strip profiles. As reference the same forming process with a conventional forming tool was carried out.

Keywords: Dry Deep Drawing, Tribology, Carbon Based Coatings, Laser Based Modification

1 Introduction and methodology

Dry sheet metal forming is mainly motivated by ecological and economical aspects [1]. The abandonment of lubricants leads to increased friction and distinctive wear. In the project ‘Lubricant free forming with tailored tribological conditions’ within the DFG priority program SPP1676 the resulting challenges in the deep drawing process are faced by the concept of a tailored tool with locally adapted friction conditions. For this purpose, different types of surface modifications are investigated to realize tailored tribological systems on the tool surfaces for dry deep drawing of a rectangular cup. The application of amorphous carbon coatings represents one approach of friction reduction as these coatings have positive effects regarding decreasing friction and high wear resistance [2]. In previous investigations, ta-C coatings revealed the most promising results regarding friction and wear in contact with the tested sheet materials – the mild deep drawing steel DC04 and the two aluminum alloys (AA5182, AA6014) [3]. Certain friction reduction compared to blank tool surfaces was achieved by a-C:H coatings due to reduction of adhesions, too. A-C:H coatings show higher adhesion strength than ta-C coatings [4]. The plasma assisted chemical vapor deposition (PACVD) process, which is used to deposit this coating type, is enhanced. In this study, the deposition parameters of substrate bias voltage and process temperature are correlated with the coating properties. The coating topography and thickness as well as mechanical and structural properties are

*E-mail address of corresponding author: Jennifer.steiner@fau.de

evaluated and represent the basis for pre-selection of coatings for strip drawing tests, later on (Fig. 1).

The minimum roughness of the ta-C and the a-C:H coatings was investigated by the variation of the machining processes which are applied before and after coating deposition [5]. Therefore, the cold working steel (1.2379) samples were polished prior to the deposition and afterwards the coatings were brushed or polished. For better understanding of the effect of the coating surface topography on the tribological behavior different surface states were evaluated by applying selected pre- and post machining processes in current investigations. Thus, the necessary surface condition is determined to achieve favorable tribological properties in terms of low friction and minimum wear. Furthermore, these investigations focus on the identification of the technologically necessary chain for pre-machining and post treatment of the deposition process. Polishing and brushing are investigated as mechanical machining processes. Due to its potential of remaining mechanical coating properties, alternatively, ultrashort pulsed laser based smoothing is applied. The ta-C coating type was selected for first finishing experiments. The effect of different mechanical machining processes on the tribological performance is examined in flat strip drawing tests (Fig. 1).

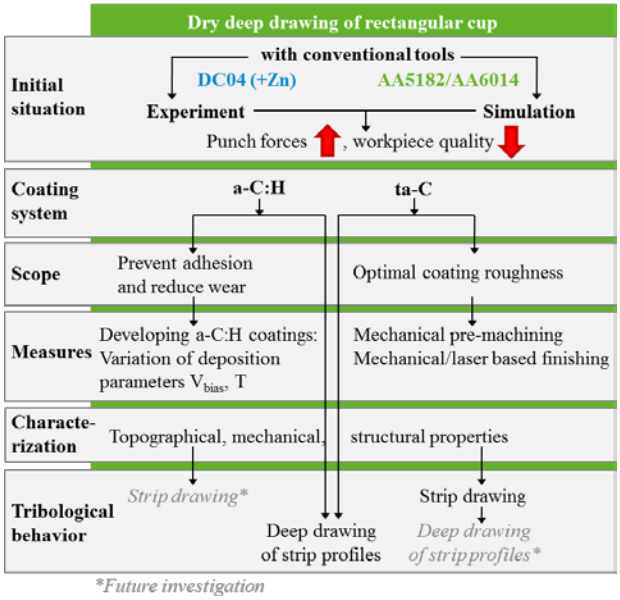

Fig. 1: Methodology of current investigation

The necessity of the local application of these surface modifications was analyzed by means of the selected model deep drawing process of a rectangular cup. The process parameters and results of the dry deep drawing process - the punch force and the stroke - are compared to those achieved by conventional deep drawing with lubricant as well as those determined by the numerical simulation of dry deep drawing. After the development and improvement of surface modifications, selected ta-C and a-C:H coatings were each investigated in dry deep drawing of strips. In this second tribological test the surface modifications are applied on the different tool segments. Each of the tested coating surfaces are mechanically post treated by brushing. Fig. 1 shows the methodology of the current investigations presented in this study.

2 Materials and test setups

Deep drawing of rectangular cups and strip drawing tests were performed within this study to analyze the tribological behavior of directly interacting tool and sheet surfaces. The cold working steel 1.2379 hardened to 60 HRC was chosen as tool material. The mild deep drawing steel DC04 and the two aluminum alloys AA5182 and AA6014 with an initial thickness of 1 mm were selected as sheet materials. Under conventional forming conditions the pressure in the flange area is varied in a range from 1 up to 10 MPa [6]. Due to high friction forces in the flange under dry conditions, the normal contact pressures during deep drawing and strip drawing tests was varied between 1.5 and 4.5 MPa depending on sheet geometry and material. Before any tests were performed, basic lubrication and soil were removed from the blanks using an acetone bath.

2.1 Forming process for analyzing dry deep drawing

In order to analyze the feasibility of dry deep drawing processes, forming of rectangular cups was analyzed with numerical and experimental methods. The deep drawing process was analyzed with the finite element software LS Dyna using an explicit modelling approach. The scope of the numerical investigation was to identify the loads and process parameters under dry and lubricated conditions. The symmetry of the workpiece was used to reduce the computation time by generating a 90°-model. As element type square shell elements with a minimal length of 1 mm are used for the blank. The material properties were modelled using the yield criterion Barlat 2000 with the values determined in [7]. The tools were modeled as rigid bodies. A variant simulation was computed upfront of this study to determine tool radii, blank layout and blank holder forces. The process design and geometry is shown in Fig. 2. A variant simulation was performed with different tool radii to find a compromise between challenging cup geometries and moderate tool loads. Therefore, the punch front end radius was set to 5 mm, whereas the die radius amounts 10 mm. The corner radius was chosen to 18 mm. The contact pressure in thke flange area is set to 4.5 MPa for DC04 and 1.5 MPa for AA5182 and AA6014. The tribological behavior was modelled by using the Coulomb friction law.

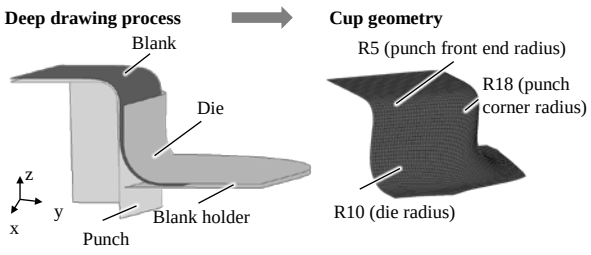

Fig. 2: Dry deep drawing model process

In accordance with the numerical model, a deep drawing tool was designed and manufactured. In a first

step, the tool surfaces and influence of modifications were analyzed globally. In further project steps, the tool surfaces will be altered locally. In order to realize this local adaption of surfaces properties, the tool is divided in several segments. The overall tool layout is shown in Fig. 3. The tool is mounted in the hydraulic press TSP100So from Lasco in order to perform the deep drawing experiments.

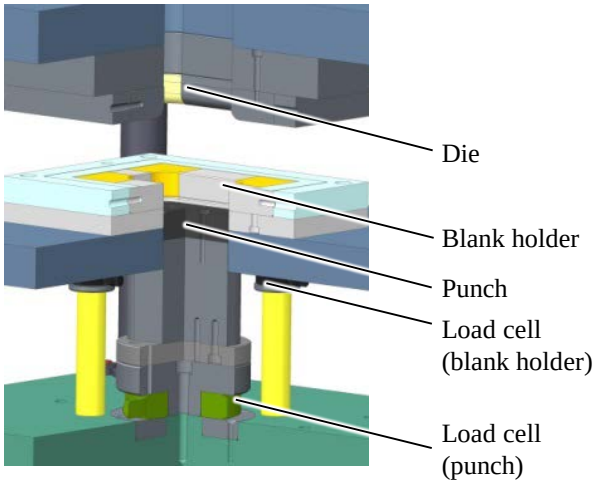

Fig. 3: CAD model of deep drawing tool

2.2 Laboratory test setup for quantification of tribological conditions

Two-sided strip drawing tests were selected to determine friction coefficients in an environment close to real forming processes. The flat strip drawing test (Fig. 4) models the tribological conditions of the flange area of a deep drawing process. A sheet metal strip is located between an upper fixed and a lower movable friction jaw which applies a defined normal force. During drawing of the strip, the necessary drawing force is recorded. By applying the Coulomb friction law the friction coefficient μ is determined as relation of drawing force to normal force. The friction jaws measure 100 mm x 55 mm. To ensure that the cutting edge of the strips are not in contact with the tools, the sheet metal strips have a width of 65 mm.

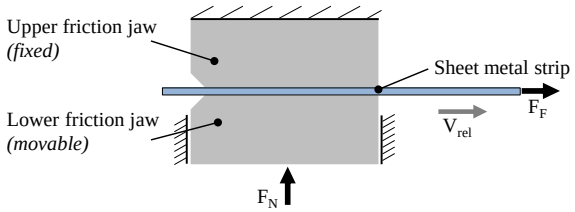

Fig. 4: Principle of flat strip drawing test

3 Results and discussion

3.1 Deep drawing with conventional tools

Dry deep drawing of rectangular cups was numerically and experimentally investigated for the different sheet materials. In a first step, the polished tool surfaces were not modified in regard of their tribological behavior. As a reference, lubricated blanks are formed to rectangular cups. For these tests, a lubricant amount of 2.0 g/m² was applied on both blank sides before forming. The force-stroke relation for the three sheet materials is summarized in Fig. 5. In addition to the experimental results, the numerically determined curves are shown. At the beginning of the deep drawing process, bending and stretch forming of the sheet are predominant until a stroke of around 5 mm. During this process phase the varying tribological conditions have no influence on the required forces. When the sheet is in contact with die and punch radii, dry conditions lead to a significant increase of punch forces. Due to lower friction, lower punch forces are achieved when lubricants are applied.

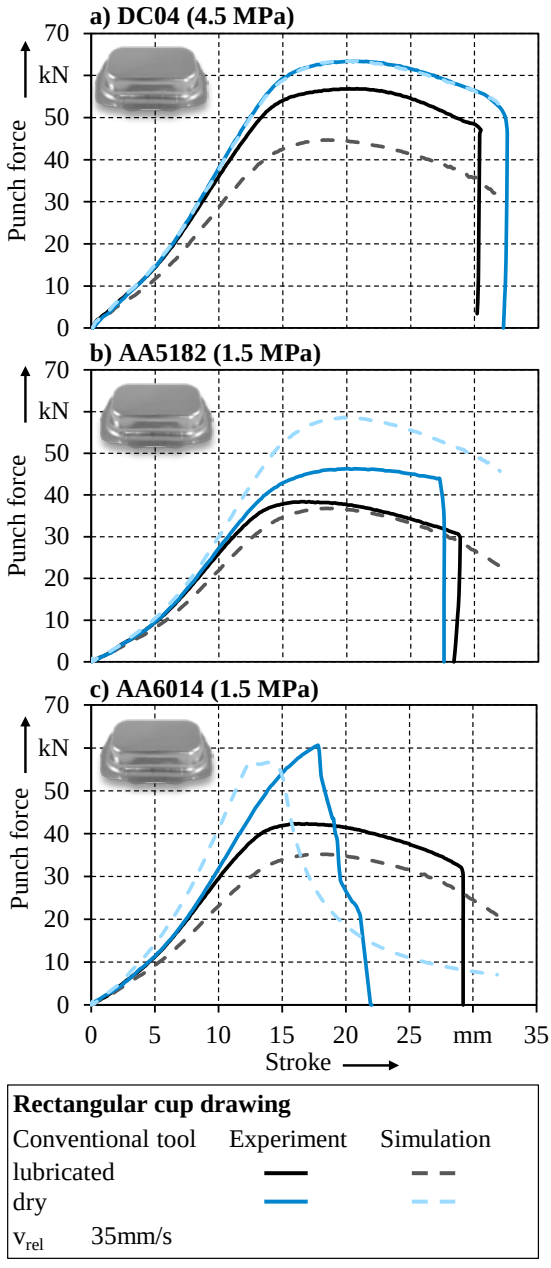

Fig. 5: Experimental and numerical force-stroke relation for lubricated and dry rectangular cups for a) DC04, b) AA5182 and c) AA6014

The maximum punch forces for DC04 are higher than those for the aluminum alloys because of higher contact pressure in the flange area and higher strength of the steel. For DC04 the maximum force increased by only 11 % compared to the lubricated reference and

rectangular cups could be drawn without cracks or severe damage of the sheet surface. This result is in good accordance with prior performed the strip drawing tests where friction increased from about 0.04 to 0.20 under dry conditions for DC04 and no wear occurred [7]. In contrast, for the aluminum alloys the friction coefficients increased more than fifteen times from about 0.02 (lubricated) to between 0.3 to 0.57 (dry) and adhesion revealed under dry conditions. Using AA5182, the maximum punch force increased from 38 to 45 kN. Without lubrication, no cracks but significant score marks occurred especially in cup edges. An even worse tribological behavior was measured when AA6014 was drawn without lubrication. The punch forces increased by 43 % and cracks occurred after 18 mm stroke. The high friction coefficient which prevents material flow from the flange area into the cup wall is the reason for the premature failure. The differences between the three materials are in good accordance with the previously investigated tribological behavior under dry conditions in strip drawing tests [7]. The results revealed that without lubrication the highest friction coefficients occur for AA6014 of about 0.57 whereas AA5182 and DC04 showed lower friction coefficients of roughly 0.3 and 0.2 respectively. These friction coefficients were used for numerical simulation of the dry deep drawing process. In contrast to both aluminum alloys, the results of the numerical force-stroke relation of DC04 are in accordance with the experimental ones (Fig. 5 a)). Reason for the deviation between simulation and experiment is the adhesive wear of aluminum and thus locally changed tribological conditions which are not considered in the numerical model. For AA5182 a 20 % higher punch force is predicted because during the long drawing length in the strip drawing tests more adhesion occurred in comparison to the deep drawing process. Therefore, the experimentally determined friction coefficient which was implemented in the numerical simulation was too high. The same reasons lead to a premature prediction of cracks for AA6014. Comparing the numerical and experimental results of lubricated tests the maximum force differs between 8 to 20 %. Reason for the higher variance might be the higher scatter during a manual application of lubricants and the distinct dependency of tribological behavior of lubricated contacts on process parameters like velocity and contact pressure. Due to the constraints of the laboratory tests, the friction coefficients in the strip drawing were determined at higher velocities and lower contact pressure than those occurring at the die radius during deep drawing. However, depending on the possibility to mirror the tribological load conditions exactly in the strip drawing tests, a high predictability of the numerical model can be achieved. The general modelling approach and material models seem to be appropriate for the simulation of the deep drawing process. Deep drawing under dry conditions with conventional tools revealed increased drawing forces and depending on the sheet material poor quality of the cup surfaces, crack formation and high wear. Especially for AA5182 and AA6014 critical forming conditions were observed according to Fig. 5. Not only increased forming forces and poor cup quality but distinctive adhesive tool wear reveals for aluminum alloys under dry conditions. The tool-sided adhesion is exemplarily shown in Fig. 6 for the die surface after dry deep drawing of AA5182.

Die surface after dry deep drawing of AA5182

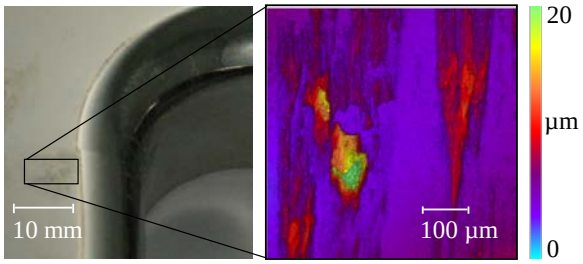

Die surface topography	
Lens	20x
Alignment	2nd degree polynomial
$n_{measurment}$	1

Fig. 6: Adhesive wear of die surface after dry deep drawing of AA5182

3.2 Investigation and development of tool-sided surface modifications

Direct contact between tool and sheet leads to increased friction and adhesion tendency. Therefore, developing and applying tool surface modifications which prevent initial wear are necessary for the realization of lubricant free deep drawing. As modifications carbon based coatings were investigated. In a first step, the effect of the topography on the tribological conditions was analyzed. The tool roughness significantly influences friction. Therefore, a new, laser based surface finishing strategy was investigated. Besides the topographical conditions, the coating properties might influence the tribological behavior. Thus, ways to adapt coating properties by variation of deposition parameters were analyzed in a last step.

3.2.1 Tribological behavior of coated tools

Former experiments revealed that carbon based coatings are suitable to decrease friction and adhesion under dry conditions [8]. Especially for both aluminum alloys the friction coefficient was reduced significantly using ta-C and a-C:H coated tools. However, the level of friction and wear reduction depends significantly on the surface roughness of the coated tools. First investigations on the influence of the coating roughness on the resulting tribological conditions in contact with AA5182 were presented in [10]. The coating process leads to a distinct surface roughening. Roughness increases due to elevated temperatures during deposition, the formation of carbon clusters and inhomogeneous growing rates at peaks and valleys. Therefore, a post treatment of coated surfaces is commonly applied to reduce the peak height. The tribological influence of the surface treatment before and after coating deposition is depicted in Fig. 7.

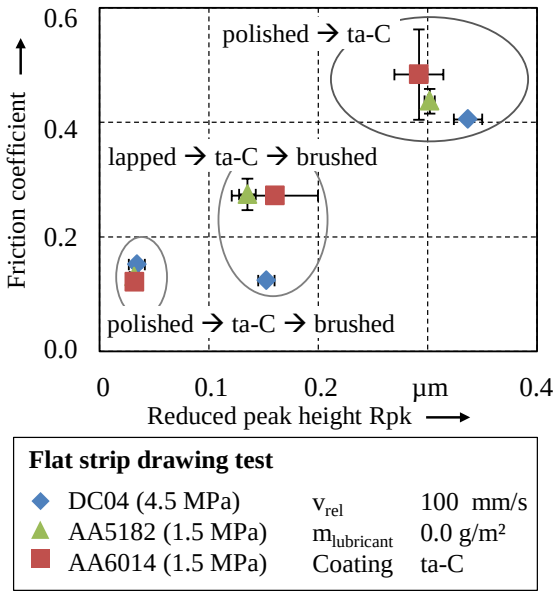

Fig. 7: Relation between reduced peak height Rpk and resulting friction coefficient µ for ta-C coated tools with varying surface treatment

The ta-C coating was applied on either lapped or polished surfaces without preferential direction of the topography. The lapped surfaces reveal a mean roughness depth (Rz) of around 0.9 and reduced peak height (Rpk) of about 0.12 before coating. In contrast, the polished surfaces show Rz and Rpk values of 0.16 and 0.02, respectively. After coating application, the difference of roughness between initially polished and lapped surfaces remained with five to seven times lower Rpk values for polished tools roughly the same. As a commonly used post surface treatment brushing was selected. Overall, three different types of surface finishing strategies were analyzed. For two process chains the friction jaws were polished before the coating deposition. Afterwards, for one of the strategies brushing was conducted. The other friction jaws were tested directly without post treatment. The third process chain consists of lapping before the coating deposition and brushing afterwards. The tribological behavior was analyzed in strip drawing tests in contact with DC04 and both aluminum alloys. The friction jaws with the lowest reduced peak height of about 0.03 µm revealed the lowest friction coefficients of 0.12 for the aluminum alloys and 0.15 for DC04. Furthermore, the lowest standard deviation for roughness and friction was measured. Applying ta-C coated jaws with Rpk values of about 0.15 µm results in a more than two times higher friction for AA5182 and AA6014. For DC04 the level of friction remains roughly the same. However, an increased abrasion of the zinc coating was observed during visual inspection. Without post treatment of the friction jaws, the Rpk value amounts about 0.30 µm and an increased standard deviation. With these tool surfaces, the friction coefficients increased to 0.4 to 0.5 for all sheet materials. For AA6014, friction coefficients above 0.5 are achieved as well with uncoated tools with Rpk values of around 0.12. For AA5182 and DC04 the friction coefficient of 0.44 and 0.40 respectively are even higher than for uncoated tools under dry conditions. One reason for the higher friction is the even higher Rpk value of 0.30 for the coated but not brushed jaws compared to 0.12 in the uncoated test series. Another reason might also be the increased hardness of the roughness asperities of coated tools which lead to a more intense mechanical interaction at dry contact surfaces. For AA6014, the small variation of friction coefficient comparing not brushed coated jaws with uncoated ones seems reasonable because the friction coefficient is already close to the maximum possible coefficient of 0.57 according to the von Mises load criterion. This investigation proofs the necessity of an adequate surface treatment in order to achieve beneficial tribological behavior. For ta-C coatings applied in dry deep drawing processes a sequence of polishing, coating and brushing is recommended as process chain. Due to their strong influence on the resulting friction, more advanced surface finishing processes will be discussed in chapter 3.2.2. Applying the same surface finishing strategy, a-C:H coatings were investigated additionally in strip drawing tests. Friction coefficients between 0.16 and 0.17 were determined for the three sheet materials. Thus, even with similar surface properties the tribological behavior of ta-C coatings slightly outperform the a-C:H coatings. Therefore, the coating properties of a-C:H coatings need to be further developed. The parameters of coating deposition influencing the coating properties will be presented in chapter 3.2.3.

3.2.2 Ultrashort pulsed laser finishing of carbon-based coatings

Laser based post machining was investigated as an alternative approach to the before mentioned mechanical post treatment processes of ta-C and a-C:H coatings. Ultrashort pulsed laser based ablation offers the opportunity of smoothing the coating surface due to nearly cold material removal. This approach has been previously investigated to reduce the average roughness on dielectrics [9]. Furthermore, applying a laser based process would have the advantage of no mechanical modification of the coating compared to the previously discussed mechanical finishing processes due to contactless processing. Finally, the reproducibility of the adjusted roughness parameters might be higher than for mechanical machining processes such as polishing due to the absent wear of the laser representing the finishing tool.

The laser finished ta-C coating was polished before the coating process but no mechanical post treatment was applied after layer deposition. The ta-C coated surface has the reduced peak height $Spk = 0.14 \pm 0.02$ µm which is higher than for additionally brushed surfaces (chapter 3.2.1). For laser finishing with a Gaussian intensity profile low peak fluence and low pulse frequency were applied to avoid accumulation of the minimum residual heat in the coating. Otherwise induced structural changes of the coatings could affect the tribological behavior, e.g. graphitization could increase the friction coefficient [3]. For this reason, the wavelength dependent thresholds of

graphitization and ablation of the ta-C coating were investigated at the pulse frequency f_P =1 kHz according to the zero-damage-method [11]. Therefore, the squared width of graphitized or ablated regions of laser processed lines was evaluated (Fig. 8). Threshold determination is the basis for the choice of peak fluences for the areal laser based smoothing process. For this, peak fluences slightly above the ablation threshold or even below the graphitization threshold can be applied. As the ta-C coating has a bandgap of about 2.6 eV corresponding to a wavelength of 477 nm, a wavelength of $\lambda = 355$ nm was applied to process the ta-C coating. This linear absorption leads to a short penetration depth and thereby to smooth material ablation.

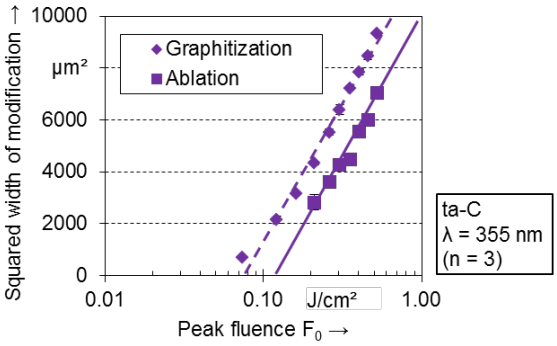

Fig. 8: Graphitization and ablation threshold for non-finished ta-C coating at $\lambda = 355$ nm ($f_P = 1$ kHz, $v_S = 200$ mm/s)

The peak fluence $F_0 = 0.070$ J/cm² slightly below the graphitization threshold was applied for ta-C surface smoothing to investigate the influence of hatch overlap Ω_y (perpendicular to scanning direction) on material removal while the pitch overlap (in scanning direction) was kept constant. The coating thickness of about 0.5 µm should be maintained by applying this peak fluence, therefore minimal material removal is favored. These investigations were carried out at a pulse repetition rate of $f_P = 40$ kHz with a fixed focusing lens (f = 150 mm) and spot diameter $d_S = 132$ µm. The sample was moved by means of linear stages (Fa. Aerotech) which enable the applied maximal speed $v_S = 200$ mm/s. As shown in Fig. 9a the pulse overlap Ω_y had no influence on the reduced peak height. Compared to the initial non post treated ta-C surface Spk was decreased by about 40 %. As the surface height of the laser processed area compared to the untreated surface (Fig. 9 a)) remains constant, laser based smoothing is induced by local removal of roughness asperities. These asperities probably consist of graphite agglomerations which have a lower ablation threshold.

Constant sp^2/sp^3 ratio which is characteristic for no graphitization and respectively sufficiently low heating of the ta-C coating is an additional requirement for laser based smoothing. This ratio was evaluated by Raman spectroscopy measurements to investigate the effect of possible heat accumulation. By the variation of the pulse frequency between 0.1 and 40 kHz different residual heats were induced. The pulse overlap $\Omega_y = 77$ % was chosen to enable minimal processing time. The number of pulses per area was kept constant by scaling the speed of sample movement and pulse frequency so that the pitch overlap Ω_x was constant. The reduced peak height does not show significant influence of the varied pulse frequency (Fig. 9 b). Furthermore, the results can be compared to the results which were achieved by applying a parameter set for generating micro features. The presented Spk of the bottom of this micro feature (Fig. 9b) − generated with $F_0 = 0.96$ J/cm² at $f_P = 40$ kHz − is roughly the same. However, the coating thickness was reduced due to material removal of about 0.25 µm depth.

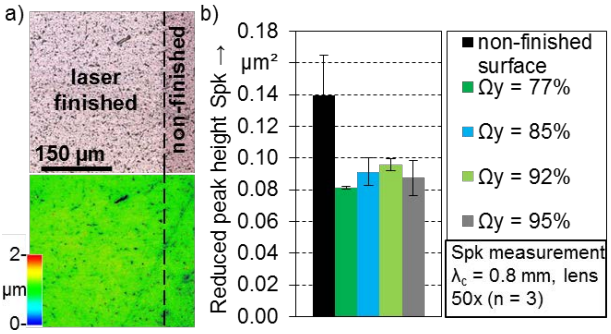

Fig. 9: a) Top view and topography of locally laser finished ta-C surface ($\Omega_y = 77$ %) as well as b) reduced peak height Spk of laser finished ta-C coatings depending on the pulse overlap Ω_y ($f_P = 40$ kHz, $v_S = 200$ mm/s)

The evaluation of the Raman spectra of the surfaces smoothed at different pulse frequencies showed that the I_D/I_G-ratios and FHWMs of the G-peak are roughly the same for the applied peak fluence $F_0 = 0.070$ J/cm². Thus, the small amount of heat input only leads to slight structural changes of the ta-C compared to the non-finished reference (Fig. 10). In contrast, the textured structure bottom showed significantly increased I_D/I_G-ratios (Fig. 10 a)) respectively decreased FHWM of the G-peak (Fig. 10 b)) which indicates undesired partially graphitization of the ta-C coating.

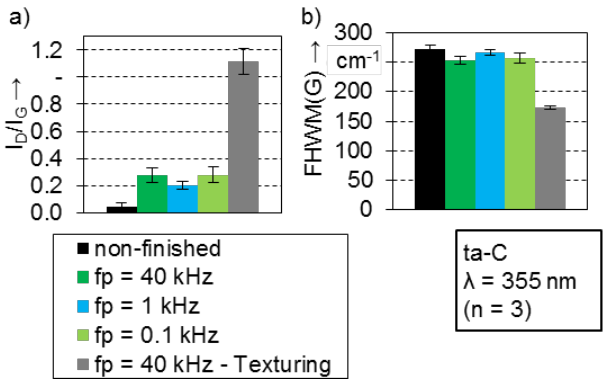

Fig. 10: Results of Raman spectroscopy of ta-C coatings

Consequently, the parameter set with the maximum investigated pulse frequency $f_P = 40$ kHz and $F_0 = 0.070$ J/cm² is suited for roughness decrease with minimum structural changes. The effect of these changes on the tribological behavior will be investigated in strip drawing tests in further studies.

3.2.3 Advanced development of a-C:H coatings

To improve the tribological behavior of a-C:H coatings the deposition process parameters and their

influences on the coating properties were further analyzed in this part of the study. The aim is that the desired coating properties can be achieved by selective adjustment of bias voltage and temperature. Furthermore, the coatings with adjusted properties ensure a specific investigation of each parameter, which may strongly affect the friction and wear during sliding. To realize this aim, the effect of each deposition parameter on coating growth rate, structure and properties was investigated systematically.

In previous work [3], the effects of deposition precursor gases on coating properties were systematically investigated. In this work, the effects of coating deposition conditions on essential coating properties, e.g. deposition rate, adhesion, hardness and indentation modulus were investigated – process temperature and substrates bias voltage – according to one-factor-at-a-time method. Since this method cannot consider two or more variables simultaneously, the multiple-factor interactions must be verified and discussed, additionally. The process temperature has great impact on the coating structure and growth procedure. In the coating growth model according to Movchan and Demchishin [12], the coating structure was found to become more dense and crystalline as the substrate temperature increases. Furthermore, an increasing temperature results in reduction of compressive residual stress and thus better adhesion [13]. The negative bias voltage is well known for its impact on coating properties such as hardness, modulus, growth rate and the ratio between sp2- and sp3-orbitals [14]. Thus, the coating properties, which are associated with tribological behavior under dry sliding conditions, are possible to be specifically adjusted by varying bias voltage.

The a-C:H coating samples were deposited using plasma assisted chemical vapor deposition (PACVD) on substrates of tool steel. The applied power supply was a unipolar voltage with 40 Hz and 5 µs. The substrates were polished using 9 µm and 3 µm diamond suspension until $Rz = 0.19 \pm 0.04$ µm and $Rpk = 0.04 \pm 0.01$ µm. Prior to the coating process the polished surfaces were cleaned with isopropanol and acetone each for 10 minutes and 2 minutes in ultrasonic bath. Then the steel substrates were kept in a vacuum oven at 80°C, in order to remove humidity and air molecules, which are adsorbed on the surface. The intended coating system consisted of a chromium adhesive layer, a tungsten carbide interlayer and the a-C:H function layer. Avoiding sharp gap between two layers, a transitional layer was added with gradually changing parameters between two layers. The detailed deposition process and applied techniques are described in Table 1. Acetylene (C_2H_2) was applied as precursor gas, which was mixed with argon (Ar). The ratio and total gas amount were investigated in previous work [15]. For the present experiment, acetylene and argon were remained generally constant at 166 sccm and 34 sccm, respectively, since a higher total gas amount or lower C_2H_2/Ar ratio results in reducing in hardness and modulus. The temperature was investigated over the range of 80 °C to 140 °C with constant bias voltage of 550 V. The highest level of temperature was kept at the same temperature at which the WC-interlayer was deposited. The lowest level was stored temperature of steel substrate in vacuum oven prior to the coating process. The bias voltage was adjusted over a wide range from 450 V to 950 V, under which a stable deposition process was ensured. In this case, the temperature was kept constant at 80°C. The level of 950 V was chosen, since a higher bias voltage led to over-heating of substrate, e.g. a bias voltage of 1200 V led to an actual deposition temperature of 120-130°C although the nominal temperature was set to 80°C.

Tab. 1: Deposition procedure and applied techniques

Step No.	Operation	Time in s	Action description
1	Heating	2400	Reactor heated to 250°C
2	Etching	2400	Reactor etched with argon at 200°C
3	Depositing interlayer	300	Vacuum arcing of Cr-Target at 180°C
4	Depositing interlayer	1080	Magnetron sputtering of WC-Target at 140°C
5	Depositing function layer	8250	PACVD process at adjusted temperature and bias voltage

After deposition, the coating samples were characterized regarding coating thickness and adhesion to substrate using calotte grinding method and Rockwell C adhesion test, respectively. Hardness and indentation modulus were measured by micro hardness indentation according to [16]. For measurements with small standard deviations all coated surfaces were post treated mechanically with 3 µm and 1 µm diamond suspensions each for 15 minutes. The chemical bonds were analyzed using Raman spectrometer with 532 nm green laser at 5 mW. The details of measurement methods and parameters were described in [3]. The a-C:H function layers deposited under 80 °C to 140 °C have a thickness of 2.3 µm to 2.5 µm. No relationship was observed between deposition rate and temperature. All the coating samples have an adhesion of HF4, which represents a sufficient adhesion with small cracks and delamination around the Rockwell indentation according to [17]. Fig. 11 summarizes the micro hardness and indentation modulus of coating samples deposited at varied temperatures.

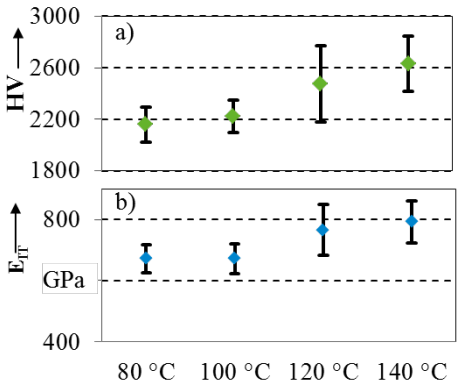

Fig. 11: a) Vickershardness and b) indentation modulus of samples deposited at different temperatures

The average Vickers hardness HV and indentation modulus E_{IT} values increase slightly with the temperature. Samples deposited at 120 °C and 140 °C show higher standard deviations of hardness and indentation modulus than those deposited at lower temperatures. Fig. 12 shows the surface topographical information of samples deposited at 80°C and 140°C before and after polishing. The surfaces were analyzed using laser scanning microscope with 20x magnification. With increasing process temperature more coating defects started to grow on the surfaces. Some coating grains and roughness asperities, which were grown on chromium droplets from vacuum arc process, were completely removed by the polishing process. This led to holes in the coating after polishing which is depicted in Fig. 12. This discontinuous coating structure also results in great fluctuations in hardness and indentation modulus. Furthermore, more roughness asperities on the sample deposited at 140 °C after the same polishing procedures due to its higher hardness are observed, which results also in big standard deviation. Although the hardness and modulus increase in average, the H/E_{IT} ratio remains unchanged and independent on temperature at 3.3.

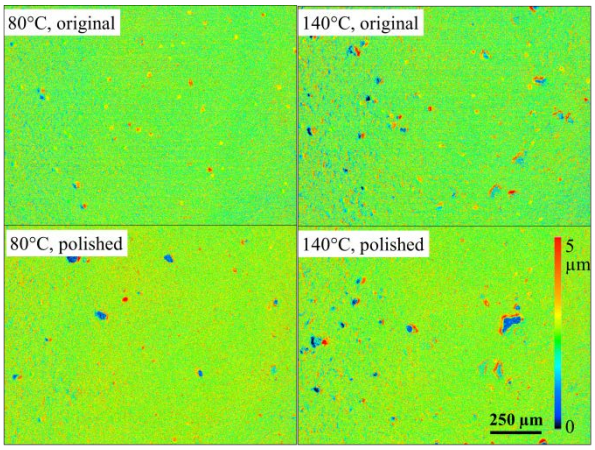

Fig. 12: Topographical information of a-C:H surfaces of 80°C and 140°C before and after polishing

Fig. 13 summarizes the coating thickness of the a-C:H function layer as a function of bias voltage. For the constant deposition time, the coating thickness increased with increasing bias voltage.

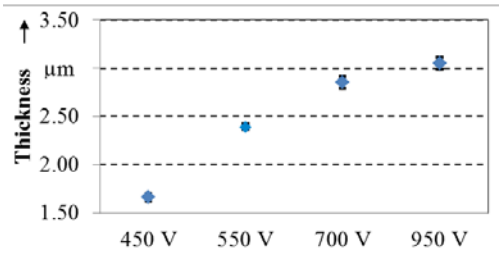

Fig. 13: Dependence of thickness of a-C:H function layer on bias voltage for each 5 repetitions

The energy-rich ionic species at higher bias voltage supported the growth process. The growth rate per every increased 100 V is smaller, because the coating structure has to overcome the side effect through strong ion bombardment. Another observed side effect is over-heating of the substrate, e.g. the measured actual reactor temperature was around 90 °C-100 °C if the bias was set to 950 V, which was 10° to 20°C higher than the nominal temperature of 80°C. A bias voltage of 450 V leads to better adhesion of coating to substrate of HF3, while other coatings show adhesion class of HF4. Average hardness and modulus are shown in Fig. 14. As the bias rises from 450 V to 700 V, the hardness and modulus increase. Due to the strong bombarding effect at 950 V, the coating structure was etched and a homogenous structure could not be ensured. As a consequence, the sample at 950 V shows reduced hardness and modulus. No obvious relation between bias voltage and H/E_{IT} ratio was determined which were in the range of 3.2 to 3.8.

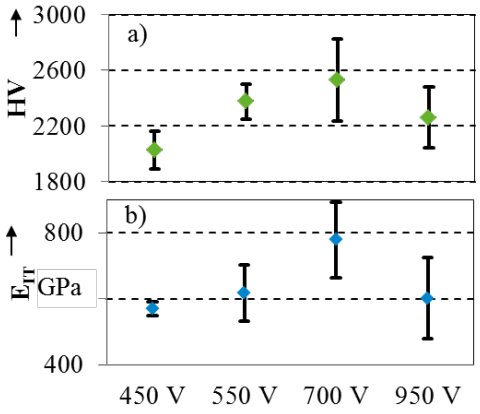

Fig. 14: a) Vickershardness and b) indentation modulus of samples deposited under different bias voltages

The chemical bonds of coating samples were analyzed by Raman spectroscopy. The I_D/I_G ratio, which is commonly used for indirect elevation of sp2/sp3 ratio between similar sample series, is shown in Fig. 15. An increased I_D/I_G ratio refers to reduced sp3 content [18]. With rising process temperature the I_D/I_G increases slightly. In contrast, another relation between bias voltage and I_D/I_G ratio is observed: a higher bias voltage results in generally higher I_D/I_G ratio, which implies that the sp3 bonds are reduced.

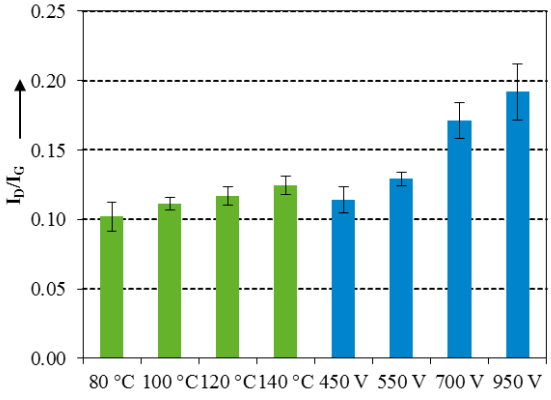

Fig. 15: Evaluation of Raman measurements of samples deposited at different temperature (green) and bias voltages (blue) with each three repetitions

Both, substrate temperature and bias voltage influence the mechanical properties and coating

structure as well as chemical bonds. A higher temperature results in an inhomogeneous and brittle coating structure which leads to spalling after polishing. The ionic species under high bias voltage with high energy accelerate the coating growth process. However, side effects including surface etching and over-heating above 700 V could not be avoided. A higher bias voltage and temperature lead to increased I_D/I_G ratio, which means lower sp3 content. H/E_{IT} could not be adjusted specifically through changing temperature and bias voltages.

3.3 Dry deep drawing with modified tool surfaces

Using the tool shown in Fig. 3 strips were deep drawn with ta-C and a-C:H coated dies and blank holders. For both coatings the tool segments were polished before the coating deposition and brushed afterwards. As a reference conventional blank polished tool surfaces were investigated. The punch was not coated in any experiment. In order to verify the general suitability of these coatings for forming tools and to proof the transferability of the flat strip drawing tests to deep drawing operations no rectangular cups but strip geometries were drawn, in a first step. Although this test setup does not mirror the whole complexity of tensile and compressive stresses of real deep drawing, it is referred to as deep drawing in this paper to mark the difference to flat strip drawing tests without forming the blank. The resulting forces for the first strip of each material are summarized in Fig. 16. The contact pressure was set to the minimum possible pressure of 4.5 MPa when using a strip width of 40 mm. Without wear the drawing force increases until the sheet is completely bend over the die and the punch radii. Afterward a constant force level is achieved during plane strain. For DC04 the maximum punch force varies in a small range between 5.0 and 5.5 kN depending on the tool surface. Due to the zinc coating DC04 has a low adhesion tendency towards the tool steel as long as the zinc coating entirely covers the substrate material. Therefore, the differences between coated and uncoated tools are not significant. However, looking at both aluminum alloys different results are observed. For AA5182 the highest forces occur for a-C:H coated tools with a maximum of around 12 kN. The force level for uncoated and ta-C coated tools reaches maximum forces of around 6 kN. The lowest level of drawing force is achieved with ta-C coated tool surface. In this case, the forces reach a constant level over the punch stroke. In contrast, for a-C:H coated and uncoated tools an increasing force over the drawing length is measured. The rising force level indicates wear occurrence. The same effect is observed for a-C:H coated and uncoated tools in contact with AA6014. After a punch stroke of 15 mm the force is still increasing. Only ta-C coated die and blank holder prevent wear mechanisms successfully. Therefore, the punch force reaches a constant level after the initial bending of the sheet. During drawing of five strips with ta-C coated segments the punch forces reveal a constant or even slightly decreasing maximum value for the three materials. Reason for the varying behavior of a-C:H coatings in contact with AA5182 and AA6014 is an interposed surface treatment of the tools due to wear occurrence. After strips out of AA5182 were drawn the a-C:H surface was worn locally. Therefore, the tools were brushed again to remove wear particles before testing AA6014. This additional surface treatment led to a lower roughness of the a-C:H coated surfaces in the tests with AA6014. Thus, lower punch forces were measured. Using a-C:H coated segments, the maximum punch force increased by 27 % for AA6014 and over 40 % for AA5182 over drawing of fives strips. Only when drawing DC04 roughly constant punch forces were measured for each strip with a-C:H coated tools.

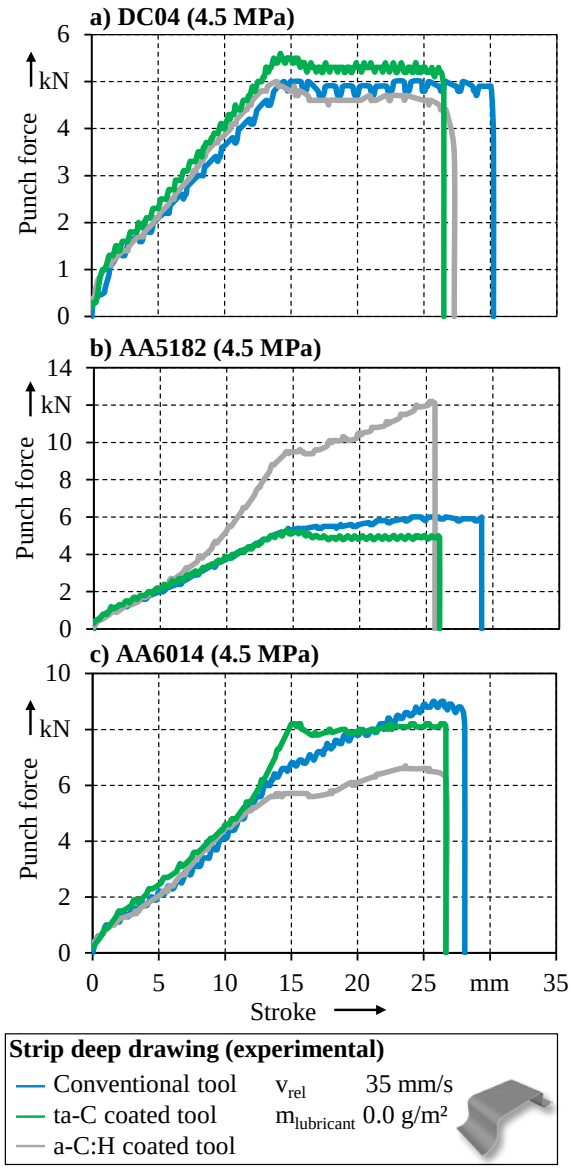

Fig. 16: Experimental force stroke relation for deep drawing strips with different tool surfaces under dry conditions for a) DC04, b) AA5182 and c) AA6014

The relation between punch force and stroke already indicates wear occurrence. Additionally, the deep drawn strips were characterized regarding their surface quality. The strips were analyzed by tactile roughness measurements. The results are summarized in Fig. 17. Distinctive grooves are observed at the strip wall. To quantify the occurrence of these grooves, the

reduced valley depth Rvk was analyzed. For each material, the drawing process leads to increased valley depth. For DC04 the results were similar for all tool surface properties. Compared to the initial sheet properties the valley depth increases from 1.7 µm to about 2.7 to 3.1 µm. The smallest grooves are measured for ta-C coated tools. However, looking at the standard deviation the differences are not significant. In contrast, for both aluminum alloys a distinct influence of the tool surface modification on the sheet surface quality is observed. In contact with AA5182 and AA6014, the lowest values of the reduced valley depth result for ta-C coated tools. The different interaction between tool and workpiece depending on the tool surface properties explain the varying progression of the force-stroke relation in Fig. 16.

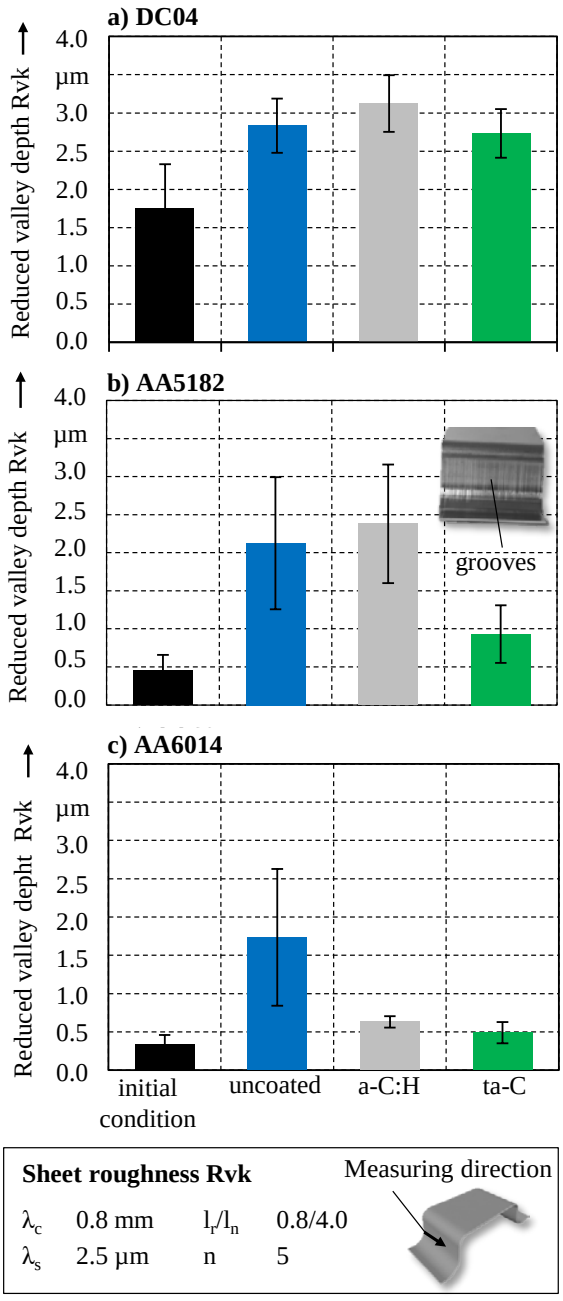

Fig. 17: Experimental force-stroke relation for deep drawing strips with different tool surfaces under dry conditions for a) DC04, b) AA5182 and c) AA6014

Overall, the force-stroke relation and the sheet surface quality indicate that the ta-C coated tool surfaces show a promising tribological behavior under dry conditions independent from the sheet material. In a next step die and blank holder will be coated completely to draw not only strips but rectangular cups under dry conditions with modified tool surfaces.

4 Conclusion and outlook

In the current study, numerical process models for deep drawing process of rectangular cups with different friction conditions were shown. From the results, a deep drawing process of zinc coated steel without lubrication is possible, which was verified by the laboratory test. However, due to severe adhesive wear deep drawing of aluminum alloys was not possible under dry conditions, both in simulation and laboratory test. At the first tool-workpiece-contact, aluminum sheet material starts to transfer to the tool surface. Amorphous carbon coatings (ta-C and a-C:H) offer a friction- and wear-reducing solution for the deep drawing process of aluminum alloys under dry conditions. Coatings with desired hardness can be produced by adjusting deposition parameters. In this work, process temperature and substrate bias voltages were investigated by one-factor-at-a-time method. Substrate bias voltage had greater impact on coating properties due to its direct influence on particle kinetic energy. A high bias voltage improves coating growth, mechanical properties and reduces sp3 content. No obvious relation between processing temperature in the range of 80-140 °C and deposition rate, mechanical properties and chemical bonds was found. Ultrashort pulsed laser based finishing enables reduction of surface asperities on ta-C coatings by local removal of the asperities. Applying a Gaussian intensity profile the reduced peak height is decreased by about 40 % compared to the coating surface without post deposition treatment. The minimized heat input leads only to slight structural changes indicated by decreased sp^3-content. The application potential of ta-C and a-C:H was evaluated through forming of a strip profile. Depending on the surface roughness, both coatings show friction- and wear-reducing effects compared to uncoated blank tools. More promising results were achieved with ta-C coated tools.

In future work, the whole blank holder and die surface will be coated with amorphous carbon and tested by forming of a complete rectangular cup. The tribological behavior of selected surface modifications as laser based smoothing and amorphous carbon coatings will be evaluated by strip drawing test. For this purpose, further reduction of heat input due to laser finishing will be investigated by the application of a top-hat shaped intensity profile. Due to shorter optical penetration depth compared to ta-C smoothing of a-C:H coatings will be investigated by applying $\lambda = 1064$ nm and top-hat profile. The evolution of the modified surfaces in small-scale for the potential applications will be verified by deep drawing of the rectangular cups.

Acknowledgement

The authors thank the German Research Foundation (DFG) for supporting the presented investigations by funding the priority program SPP 1676 project ME 2043/50-1, SCHM 2115/49-1 and TR 1043/5-1 with the project title “Lubricant free forming with tailored tribological conditions”.

References

[1] F. Vollertsen, F. Schmidt: Dry Metal Forming: Definition, Chances and Challenges. International Journal of Precision Engineering and Manufacturing - Green Technology 1(1) (2014) 59-62

[2] Association of German Engineers (VDI): VDI Guideline 2840. Beuth (2012)

[3] M. Merklein, M. Schmidt, S. Tremmel, K. Andreas, T. Häfner, R. Zhao, J. Steiner: Tailored modifications of amorphous carbon based coatings for dry deep drawing. Dry Metal Forming Open Access Journal (2015) 25-39

[4] J. Vetter: 60 years of DLC coatings: Historical highlights and technical review of cathodic arc processes to synthesize various DLC types, and their evolution for industrial applications. Surface and Coating Technology 257 (2014) 213-240

[5] Steiner, J.; Andreas, K.; Merklein, M.: Investigation of surface finishing of carbon based coated tools for dry deep drawing of aluminium alloys. IOP Conference Series: Materials Science and Engineering 159(2016)1, S. 12022_1-10

[6] A. Birkert, S. Haage, M. Straub: Umformtechnische Herstellung komplexer Karosserieteile, Springer Vieweg, Berlin Heidelberg, 179-209

[7] M. Merklein, M. Schmidt, S. Tremmel, S. Wartzack, K. Andreas, T. Häfner, R. Zhao, J. Steiner: Investigation of Tribological Systems for Dry Deep Drawing by Tailored Surfaces.Dry Metal Forming - OAJ FMT 1(2015), S. 42-56

[8] M. Merklein, M. Schmidt, S. Tremmel, S. Wartzack, K. Andreas, T. Häfner, R. Zhao, J. Steiner: Development and Evaluation of Tool Sided Surface Modifications for Dry Deep Drawing of Steel and Aluminum Alloys. Dry Metal Forming Open Access Journal (2015) 121-133

[9] J. Heberle, F. Klämpfl, I. Alexeev, M. Schmidt: Ultrafast Laser Surface Structuring of Intraocular Lens Polymers. In: J. Laser Micro/Nanoeng. 8(2) (2013) 51–55

[10] J. Steiner, K. Andreas, M. Merklein: Investigation of surface finishing of carbon based coated tools for dry deep drawing of aluminium alloys. In: ASMET (Hrsg.): Proc. Int. Deep Drawing Research Group Conf., Linz, 2016, 679-688

[11] J.M. Liu: Simple Technique for Measurements of Pulsed Gaussian-beam Spot Sizes. Opt. Lett. 7(5) (1982) 196-198

[12] B.A. Movchan, A.V. Demchishin, Study of the structure and properties of thick condensates of nickel, titanium, tungsten, aluminum oxide and zirconium dioxide, Fiz. Metal. Metalloved 28 (1969) 653-660

[13] H.W. King, J.D. Brown, T.A. Caughlin: Temperature dependence of residual stress in TiN films on 316 stainless steel. 46 Annual Denver X-ray Conference (DXC), Denver, 1997

[14] L. Ward, F. Junge, A. Lampka, M. Dobbertin, C. Mewes, M. Wienecke: The effect of Bias Voltage and Gas Pressue on the Structure, Adhesion and Wear Behavior of Diamond Like Carbon (DLC) Coatings With Si Interlayers. Coatings 2014, 4. Open Access. 214-230

[15] R. Zhao, J. Steiner, K. Andreas, M. Merklein, S. Tremmel, Investigation of Tribological Behaviour of a-C:H Coatings for Dry Deep Drawing of Aluminium Alloys, The 17th Nordic Symposium on Tribology (NORDTRIB), Hämeenlinna, 2016

[16] German Institute for Standardization (DIN): DIN EN ISO 14577. Beuth (2003)

[17] Association of German Engineers (VDI): VDI Guideline 3198. Beuth (1992)

[18] A. C. Ferrari, J. Robertson: Resonant Raman spectroscopy of disordered amorphous, and diamond like carbon. Physical Review B. 64(7) (2001) 075414